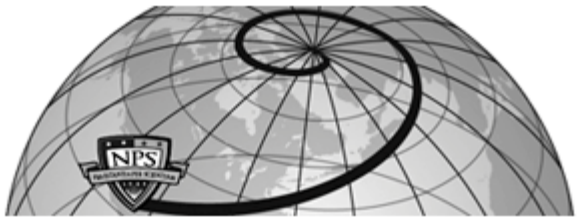

NUMERICAL PREDICTION OF PLANETARY-SCALE WAVES.

NOEL TEMPLE WOOD

NUMERICAL PREDICTION OF PLANETARY-SCALE WAVES

* * * * *

Noel Temple Wood

NUMERICAL PREDICTION OF

PLANETARY-SCALE WAVES

by

Noel Temple Wood
Lieutenant, United States Navy

Submitted in partial fulfillment of
the requirements for the degree of

MASTER OF SCIENCE
IN
METEOROLOGY

United States Naval Postgraduate School
Monterey, California

1 9 6 3

NUMERICAL PREDICTION OF PLANETARY-SCALE WAVES

by

Noel Temple Wood

This work is accepted as fulfilling
the thesis requirements for the degree of
MASTER OF SCIENCE
IN
METEOROLOGY
from the
United States Naval Postgraduate School

ABSTRACT

Current numerical barotropic and baroclinic forecasting models have shown an inability to correctly represent the behavior of the planetary-scale waves. A mathematical model, based on the thermodynamic energy equation, has been proposed by Wiin-Nielsen as a means of predicting the behavior of the planetary-scale waves. The model is programmed for the Control Data Corporation 1604 digital computer to utilize the operational output of machine-processed data and analyses produced by the U. S. Navy Fleet Numerical Weather Facility (FNWF), Monterey, California. The present form of the program yields a 1-hr planetary-scale forecast at 1000 mb, 850 mb, 700 mb, 500 mb and 300 mb in ten minutes.

The writer wishes to express his appreciation to Professor George J. Haltiner of the U. S. Naval Postgraduate School for his guidance, contributions and encouragement in this work.

Appreciation is expressed to Lieutenant Commander Mildred J. Frawley, United States Navy and Mr. Milton H. Reese of FNWF for the aid and advice in programming and performing the machine computations. Thanks are expressed to Mrs. Lillian F. Paine and Mrs. N. T. Wood for their efforts in typing this thesis.

TABLE OF CONTENTS

LIST OF ILLUSTRATIONS

TABLE OF SYMBOLS

D - the height anomaly: $D = z - \bar{z}$

H_t - the terrain height

P - the pressure difference across a vertical layer of thickness h

R - the gas constant for dry air

T - the absolute temperature

c_p - the coefficient of specific heat at constant pressure

c_v - the coefficient of specific heat at constant volume

d - the grid-net spacing distance

f - the coriolis parameter: $f = 2\Omega \sin\phi$

f_m - the coriolis parameter at latitude 45N

f_o - the coriolis parameter at latitude 90N

g - the vertical component of the acceleration due to gravity

h - the thickness of a layer between two isobaric surfaces

m - the map-scaling factor: $m(\phi) = \frac{1+\sin 60^\circ}{1+\sin\phi}$

p - the atmospheric pressure

t - time

u - the component of wind speed in the x direction

v - the component of wind speed in the y direction

w - the component of wind speed in the z direction

z - the height of an isobaric surface

β - the Rossby parameter: $\beta = \partial f / \partial y$

γ - the actual lapse rate

γ_d - the dry adiabatic lapse rate

$\Delta( )$ - the finite difference of a parameter

Δ_p - the finite-difference operator corresponding to $\partial/\partial p$

Δ_p^2 - the finite-difference operator corresponding to $\partial^2/\partial p^2$

ζ - the relative vorticity: $\zeta = \partial v/\partial x - \partial u/\partial y$

η - the absolute vorticity: $\eta = \zeta + f$

σ - the static stability parameter

ϕ - the latitude

ω - the total derivative of pressure with respect to time

∇ - the horizontal gradient operator: $\nabla = i\,\partial/\partial x + j\,\partial/\partial y$

∇^2 - the Laplacian operator: $\nabla^2 = \partial^2/\partial x^2 + \partial^2/\partial y^2$

$J(,)$ - the finite-difference operator corresponding to the Jacobian

V - the horizontal projection of the wind velocity vector

V_t - V at the terrain level

$( )_k$ - a parameter at level k. In the case of thickness, a thickness centered at level k

$( )^{(k)}$ - the k-th value of a parameter in an iterative scheme

$(\bar{})$ - a parameter in a standard atmosphere

$(\hat{})$ - a scaled parameter, less than one

1. Introduction.

Current numerical barotropic and baroclinic forecasts of the height of the 500-mb surface show an inability to correctly represent the behavior of planetary-scale waves. Early models caused these long waves to retrogress at speeds approaching the Rossby speed. This phenomenon is not observed in the atmosphere and much work has been done in an effort to correct this difficulty. Wolff [7] has shown that forecasts by the non-divergent barotropic model are more nearly correct if the planetary-scale waves are held stationary. Another approach to correct this defect has been to introduce a Helmholtz term into the vorticity equation. This is equivalent to adding a small amount of divergence. Wiin-Nielsen [5] pointed out that an analysis of baroclinic instability and phase speeds of waves in a baroclinic atmosphere leads to the conclusion that the phase speed for large wave lengths approaches the Rossby speed in a non-divergent atmosphere.

Burger [1] has shown, from scale considerations, that the vorticity equation loses its prognostic value and assumes a quasi-stationary character for waves whose lengths are of the same order of magnitude as the radius of the earth. Adopting this as a working hypothesis, and defining waves of this magnitude as planetary-scale waves, Wiin-Nielsen [6] developed a prediction model for the planetary-scale waves.

This investigation is an attempt to provide a means of correctly predicting the planetary-scale motion based on the Wiin-Nielsen model.

2. The Model.

The vorticity equation for large-scale atmospheric flow in isobaric coordinates is

$$\frac{\partial \eta}{\partial t} + V \cdot \nabla \eta + \omega \frac{\partial \eta}{\partial p} = -\eta \nabla \cdot V + \left(\frac{\partial \omega}{\partial y} \frac{\partial u}{\partial p} - \frac{\partial \omega}{\partial x} \frac{\partial v}{\partial p} \right). \qquad (1)$$

Burger [1] showed that this equation may be greatly simplified by order-of-magnitude considerations when applied to the planetary scale. Equation (1), after Burger, reduces to the stationary form

$$\beta v + f \nabla \cdot V = 0 . \qquad (2)$$

Wiin-Nielsen [6] demonstrated that equation (2) leads to instability on all scales, with large amplification rates for the smaller scale motions which may be present. The shorter waves were stabilized by adding the advection of relative vorticity into equation (2), leading to

$$V \cdot \nabla \eta + f_m \nabla \cdot V = 0$$

or (3)

$$V \cdot \nabla \eta = f_m \frac{\partial \omega}{\partial p} .$$

The coriolis parameter in equation (2) is modified to f_m in equation (3) to avoid mean-vorticity generation at any level. The inclusion of relative vorticity leads to the delineation of a region of instability. In the meteorological range of vertical wind shear and wave length, the shortest e-folding time is of the order of 5 days. The e-folding time is the time required for the amplitude to increase by a factor of e. Since the amplification rate is given by $e^{\frac{2\pi c_i t}{L}}$, the e-folding time is simply

$$t_e = L/2\pi c_i .$$

The thermodynamic energy equation is derived in a straightforward manner from the first law of thermodynamics, applied to adiabatic flow, giving

$$\frac{\partial}{\partial t}\left(\frac{\partial z}{\partial p}\right)+\nabla\cdot\nabla\left(\frac{\partial z}{\partial p}\right)-\omega\left[\frac{R}{pg}\left(\frac{\partial T}{\partial p}-\frac{RT}{pc_p}\right)\right]=0. \tag{4}$$

This equation may be transformed to equation (5) by approximating $\frac{\partial z}{\partial p}$ by finite differences.

$$\frac{\partial h}{\partial t}+\nabla\cdot\nabla h-\frac{p\sigma\omega}{g}=0 \tag{5}$$

where

$$\sigma=\frac{R}{p}\left(\frac{\partial T}{\partial p}-\frac{RT}{pc_p}\right). \tag{6}$$

To apply equations (3) and (5), the atmosphere is divided into 9 layers by isobaric levels numbered 0 to 9, where the levels 0 and 9 correspond to 200 mb and 1000 mb, respectively (see figure 1).

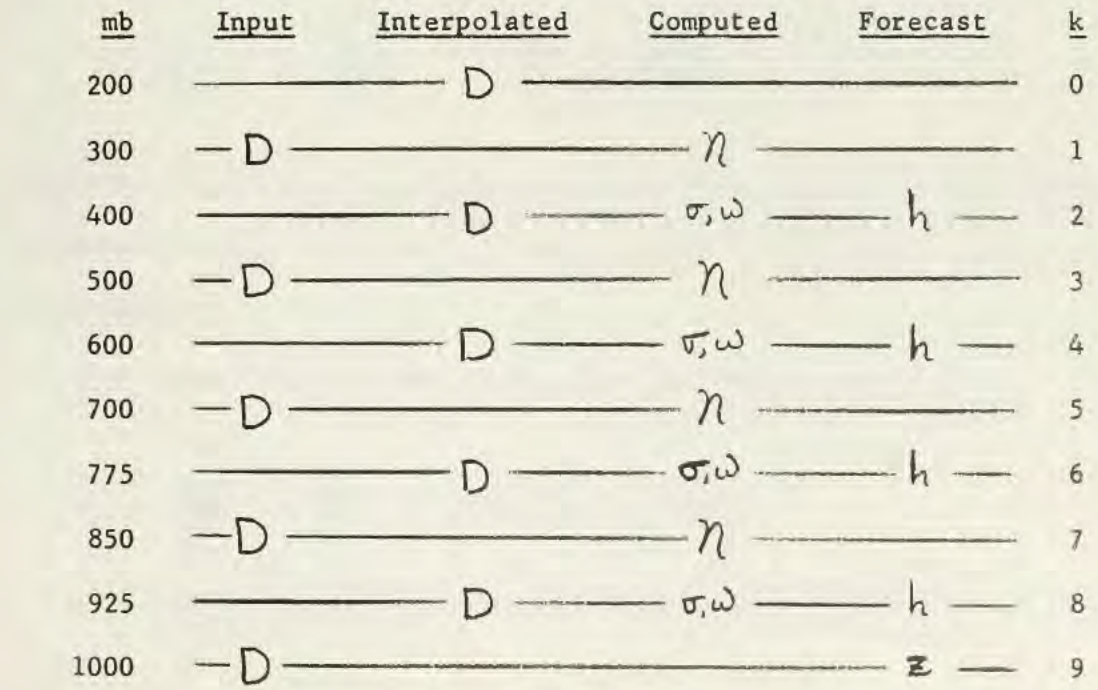

Figure 1. Level arrangement for the model.

The vertical velocity is computed at even levels by applying the vorticity equation, (3), at the odd levels as follows:

$$\omega_k = \omega_{k-2} + P/f_m \, V_{k-1} \cdot \nabla(f_{k-1} + f). \tag{7}$$

Here k is even and P is the pressure difference between even levels. The vertical velocity is assumed to be zero at 200 mb.

The prognostic equations are obtained by applying the thermodynamic energy equation, (5), at the even levels, namely,

$$\frac{\partial h_k}{\partial t} = -V_{k-1} \cdot \nabla h_k + \frac{P \sigma_k \omega_k}{g}. \tag{8}$$

Equation (6) may also be expressed as

$$\sigma_k = \frac{R^2 T_k}{p_k^2 g} (\gamma_d - \gamma) \tag{9}$$

or

$$\sigma_k = g \frac{\partial^2 z_k}{\partial p^2} + \frac{c_v}{c_p} \frac{g}{p_k} \frac{\partial z_k}{\partial p}. \tag{10}$$

Equation (9) is used to evaluate the stability parameter in a standard atmosphere at the even levels. These values are included in the program as constants.

The lower boundary condition is established by noting that

$$\omega = \frac{dp}{dt} = \frac{\partial p}{\partial t} + V \cdot \nabla_p - \rho g w. \tag{11}$$

The second term of the right hand side of equation (11) is zero in

geostrophic flow. Since w at the surface is given by

$$w = \mathbf{V}_t \cdot \nabla H_t ,$$

equation (11) may be rearranged to obtain equation (12a),

$$\frac{\partial z}{\partial t} \doteq -\omega \frac{\partial z}{\partial p} + \mathbf{V}_t \cdot \nabla H_t \qquad (12a)$$

or, approximately,

$$\frac{\partial z_q}{\partial t} \doteq \frac{\partial z_s}{\partial t} \doteq -\omega_s \frac{\partial z_s}{\partial p} + \mathbf{V}_q \cdot \nabla H_t , \qquad (12b)$$

where the surface wind, $\mathbf{V}_t$, has been approximated by $\mathbf{V}_q$. The difficulties embodied in equations (12a) and (12b) are rather serious since ω at the lower boundary is usually obtained by neglecting $\frac{\partial z}{\partial t}$ in equation (12a). Thus, it is likely that $\frac{\partial z}{\partial t}$ is a small difference of two relatively large terms. In spite of these misgivings, the initial program was designed in accordance with Wiin-Nielsen's model as approximated by equation (12b).

The computations carried out during this investigation were made with a Control Data Corporation 1604 (CDC 1604) digital computer, with a core storage capacity of 32,768 words of 48 bits each. The input data were obtained from the bi-daily analysis of the height of the 300-mb, 500-mb, 700-mb, 850-mb and 1000-mb surfaces by the U. S. Navy Fleet Numerical Weather Facility (FNWF), Monterey, California.

In order to utilize available data and computer subroutines from FNWF, the equations were converted to finite-difference form and scaled for fixed-point fractional arithmetic.

A 1977-point, square-net, octagonal grid, circumscribed by latitude 10N on a polar stereographic projection of the Northern Hemisphere, was employed to represent the data fields. The net spacing is 381 km at 60N where the projection is true.

The scaled, finite-difference equations corresponding to equations (8), (7), (10) and (12) are equations (13), (14), (15) and (16), respectively.

$$\frac{\Delta \hat{h}_k}{\Delta t} \doteq -\left(\frac{g}{f_o d^2}\right)\frac{\hat{m}^2}{\sin\phi}\,\mathcal{J}\left(\hat{D}_{k-1}, \hat{h}_k\right)\cdot 2^{17} + \frac{\hat{P}\hat{\sigma}_k\hat{\omega}_k}{g}\cdot 2^{12} \tag{13}$$

$$\hat{\omega}_k \doteq \hat{\omega}_{k-2} + \hat{P}/\hat{f}_m\left(\frac{g}{f_o d^2}\right)\frac{\hat{m}^2}{\sin\phi}\,\mathcal{J}\left(\hat{D}_k, \hat{\eta}_k\right)\cdot 2^{21} \tag{14}$$

$$\hat{\sigma}_k \doteq \hat{\bar{\sigma}}_k + \left[\left(\frac{g}{(\bar{P}_k)^2}\right)\Delta_p^2\hat{D}_k + \left(\frac{c_v}{c_p}\,\frac{g}{\bar{P}_k}\,\frac{1}{\bar{P}_k}\right)\Delta_p\hat{D}_k\right]\cdot 2^{17} \tag{15}$$

$$\frac{\Delta \hat{z}_q}{\Delta t} \doteq -\hat{\omega}_8\left(\frac{1}{\hat{P}}\right)\left(\Delta_p\hat{z}_8\right)\cdot 2^{6} + \left(\frac{g}{f_o d^2}\right)\frac{\hat{m}^2}{\sin\phi}\,\mathcal{J}\left(\hat{D}_q, \hat{H}_t\right)\cdot 2^{20} \tag{16}$$

The scaling conventions used in these equations are

$$\omega = \hat{\omega}\cdot 2^{7} \qquad (\text{mb} - \text{sec}^{-1})$$

$$f = \hat{f}\cdot 2^{-9} \qquad (\text{sec}^{-1})$$

$$D = \hat{D}\cdot 2^{17} \qquad (\text{cm})$$

$$P = \hat{P}\cdot 2^{11} \qquad (\text{mb}) \tag{17}$$

$$m = \hat{m}\cdot 2^{1} \qquad (\text{non-dimensional})$$

$$\eta = \hat{\eta}\cdot 2^{-9} \qquad (\text{sec}^{-1})$$

$$z = \hat{z}\cdot 2^{27} \qquad (\text{cm})$$

$$\sigma = \hat{\sigma}\cdot 2^{11} \qquad (\text{cm}^2\ \text{sec}^{-2}\ \text{mb}^{-2})$$

$$H_t = \hat{H}_t \cdot 2^{20} \quad \text{(cm)}$$

$$h = \hat{h} \cdot 2^{17} \quad \text{(cm)}$$

Equation (6) represents the standard stability plus an anomaly due to the departure from the standard atmosphere. The quantity $\hat{\overline{\sigma}}_k$ in equation (15) refers to the stability parameter at level k in a standard atmosphere. The remainder of the right hand side of equation (15) is the finite-difference form of equation (10), which was used to approximate the stability anomaly at each grid point. The point values of stability are averaged over each pressure surface to maintain consistency with respect to the energetics of the model.

The vertical derivatives in the calculation of the stability anomaly are approximated in a conventional manner [3, pp. 47-49]. The height fields at the even levels (figure 1) are approximated by a simple linear relationship. It is assumed that the ratio of the height of a level to its adjacent level in a standard atmosphere is the same as the ratio of the heights of these levels in the real atmosphere. A test of the validity of this assumption indicates that the standard deviation of the actual ratios with respect to the standard ratios is two orders of magnitude less than the ratios themselves. The approximation leads to a maximum error of 9% of the height in the 54 cases examined, with an average error of less than 1%. The approximation is less accurate in the lower portions of the atmosphere than it is in the upper regions below the tropopause.

Additional boundary conditions are imposed on the finite-difference approximation to the model. These include:

a) setting the forecast height and thickness changes at the grid boundary points to zero;

b) setting the relative vorticity and vertical velocity at the grid boundary points to zero.

The order of computation during a time step is as follows:

a) the previously prepared planetary-scale height analyses at the five odd levels (see figure 1) are entered into the computer and the height values at the five even levels are approximated;

b) the stability parameter is computed at each grid point on levels 2, 4, 6 and 8 and is pressure averaged for each level;

c) the vertical velocity is computed at each even level from the advection of absolute vorticity at the next lower odd level after establishing the vertical velocity at level 0 as zero;

d) the thickness fields between adjacent odd levels are obtained from the input height fields and the advection of thickness is calculated;

e) the advection of thickness and the vertical velocity term at each even level, except level 0, is combined to form the local thickness change;

f) the height change at level 9 is determined;

g) the calculated height and thickness changes are combined with the initial height at level 9 and the thicknesses of the upper layers to form the forecast height fields at levels 1, 3, 5, 7 and 9.

Forward-difference approximations are used in the initial time step. All subsequent time steps employ central differences.

3. Investigative Procedures and Results.

An initial attempt at evaluating the model was made by providing the space-mean height fields at 300 mb, 500 mb, 700 mb, 850 mb and 1000 mb as input. These fields are obtained by passing the analyzed height fields through four scans of the smoothing equation,

$$A^{(1)}_{ij} = A^{(0)}_{ij} + k\nabla^2 A^{(0)}_{ij} . \qquad (18)$$

In this instance, k = 1/8. This approach proved unsuccessful. An analysis by Holl and Clark [2] of the wave-component residuals shows that, after smoothing, 50% of the energy of wave number 16 remains in the space-mean pattern at latitude 45N. This is sufficient justification to remove the FNWF space-mean, in its present form, as a suitable input for the model under consideration.

The 1000-mb height-change forecasts produced by the approximations of equations (12a) and (12b) were unsatisfactory. The forecast changes had no pattern and were an order of magnitude larger than observed values. This result casts further doubt on the utility of equations (12a) and (12b).

A second approach was to provide the model with input fields which were prepared by a hemispheric Fourier analysis of the height fields. The zonal mean and the components due to waves 1, 2 and 3 were extracted and added together. These summed fields provided a planetary-scale input to the model. Figure 2 is a sample of one of the fields used in the limited evaluation of the model.

The first attempts with the Fourier input were not successful. Short-wave components were generated and first appeared in the mapped height fields after a 2-hr forecast. These components continued to grow

in amplitude and progressed around latitude circles, as shown in figure 3 for an 8-hr forecast. These short-wave phenomena are tentatively attributed to computational instability. The time interval used in these unstable forecasts was one hour.

The 1000-mb height-change forecast was not unstable; however, the earlier difficulties persisted. On this basis, the utility of equations (12a) and (12b) was rejected. In the interest of evaluating the main features of the model, a simple approximation to the lower boundary conditions was adopted. The 12-hr height changes at the 1000-mb surface were determined from the result of the Fourier analysis of the initial height fields. It was then assumed that the appropriate fraction of this change would be applied to the 1000-mb surface at each time step. Such an approximation leads to minor inconsistencies during the iterative procedure, but leads to a perfect 12-hr forecast at 1000 mb.

The problem of possible computational instability has been approached on the basis of the general considerations outlined by Thompson [4]. The 1-hr time interval was halved, while retaining the approximation for the lower boundary.

At the time of writing, 26 time steps have been calculated with no sign of short-wave phenomena, which appears to support the earlier suggestion of computational instability associated with 1-hr time steps. Figure 4 is a 12-hr forecast for the 500-mb level from 12Z 19 November 1962. The errors associated with this forecast are shown in figure 5. The forecast 12-hr height-change field is figure 6 and the actual 12-hr height-change field is figure 7. The analyzed 500-mb field for 00Z 20 November 1962 is figure 8. The pillow and root-mean-square error from figure 6 are very similar to those obtained from figure 7

(Pillow, P, and root-mean-square error, RMSE, are defined in Appendix I.) In figure 6, P = -2 feet and RMSE = 71 feet, while figure 7 gives P = 6 feet and RMSE = 74 feet. An examination of figure 5 shows a region of large errors in the vicinity of the North Pole (at the center of the figure). This is to be expected since the features of the input data are not of planetary scale at these latitudes. The major errors, with a maximum of -480 feet, are associated with the slightly deepening low center in the northwest region of figure 2. The model forecasts a lowering of central height to 16,560 feet. In actuality, the height lowered to 16,770 feet at the position one grid point to the northeast. Most of the other errors in the lower latitude regions are less than 100 feet. These errors appear small enough to warrant further evaluation of the model. Appendix I is a tabulation of the pillow and RMSE of error fields generated when using persistence as a forecast on selected days of November 1962. These indicate the forecast improvement required of the Wiin-Nielsen model.

4. Suggestions for Future Study.

The limited results described in section 3 are not yet adequate to evaluate the usefulness of the long-wave model. There remain several tasks to be accomplished before this may be established.

a) Revise and streamline the present computer program to reduce the amount of time required to make the calculations for one time step. At present, this time is 5 minutes; however, this may be reduced, by more sophisticated tape handling, to about 3 minutes. Further reduction might be made by packing data in the computer memory to minimize or eliminate the necessity of data transfer to and from magnetic tape.

b) Conduct an extensive evaluation of the model on many sets of data to prove or disprove the adequacy of equations (3) and (5).

c) If the evaluations of b) prove the model to be successful, a suitable lower boundary condition must be devised and tested in order to obtain operational planetary-scale forecasts. A further desirable feature for an operational forecasting model would be the elimination of the required Fourier analysis of the input data. The most likely possibility here may be the use of one of the new smoothing techniques presently undergoing test at FNWF.

Figure 2 - 500-mb height analysis of the Northern Hemisphere after Fourier analysis. 12Z 19 November 1962.

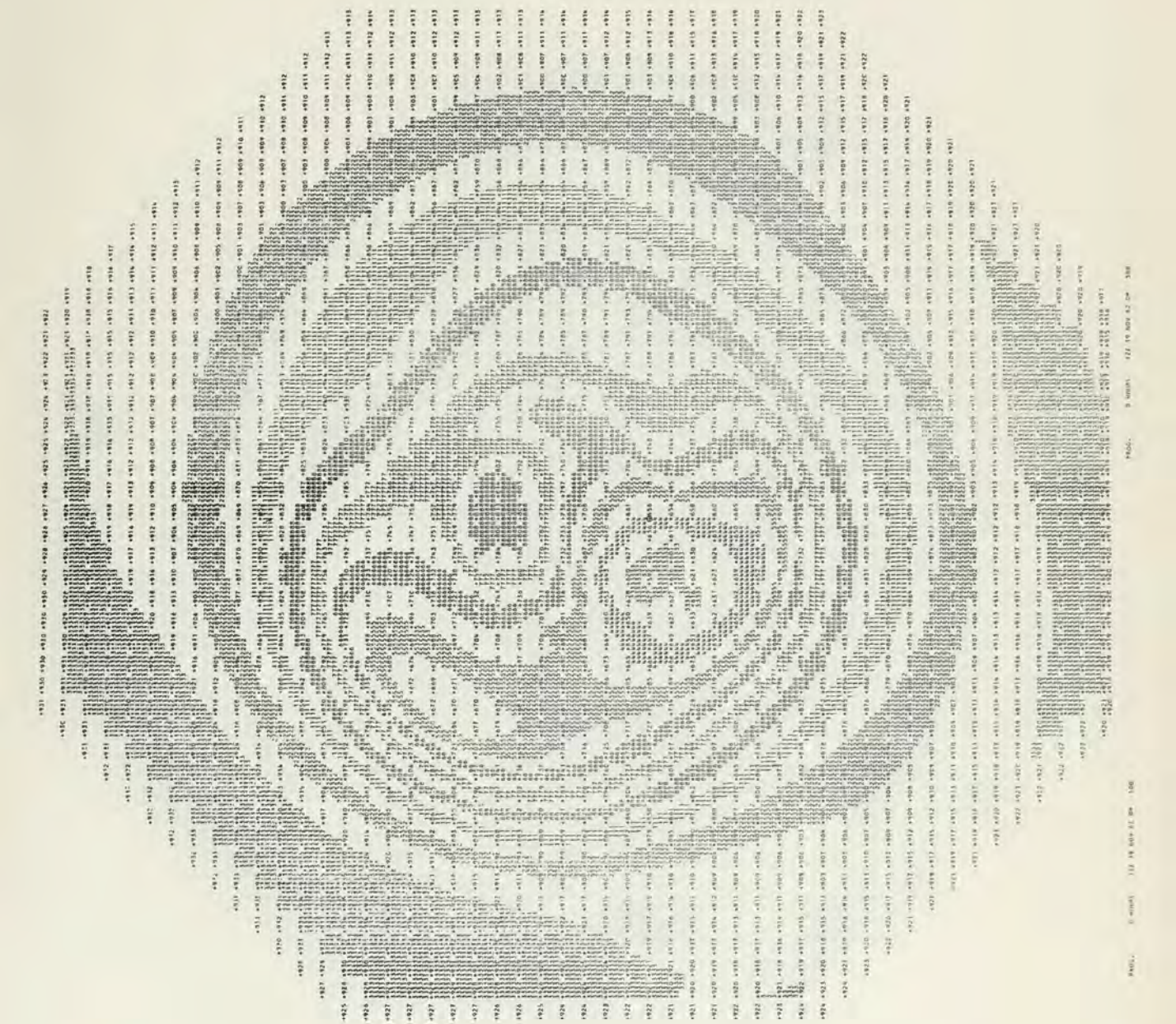

Figure 3 - 500-mb planetary-scale height forecast for the Northern Hemisphere showing features evaluated as computational instability. 8-hr forecast from 12Z 19 November 1962. 1-hr increments.

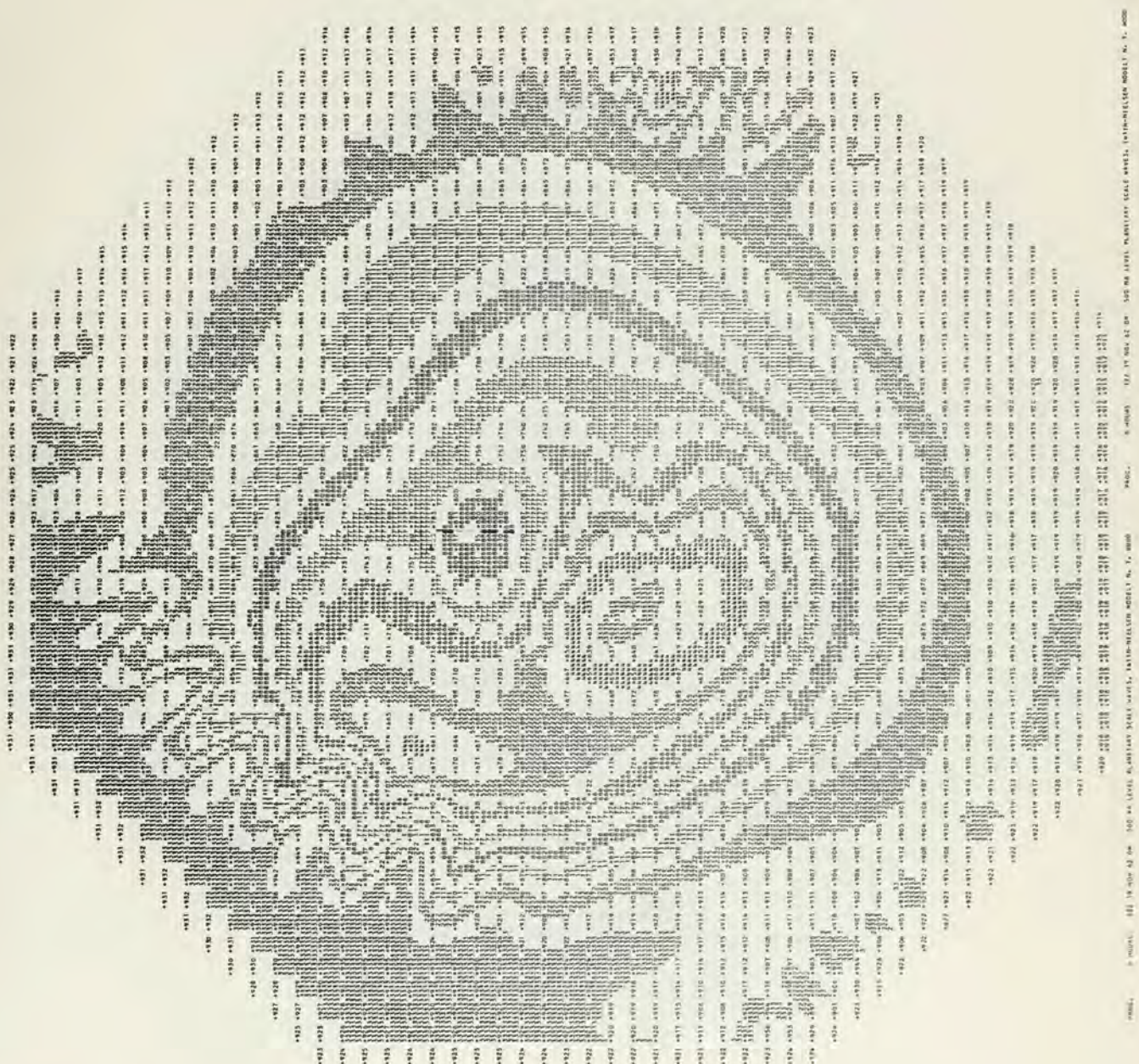

Figure 4 - 12-hr 500-mb planetary-scale height forecast for the Northern Hemisphere from 12Z 19 November 1962. 30-min increments.

Figure 5 - 12-hr 500-mb planetary-scale height-forecast errors for the Northern Hemisphere from 12Z 19 November 1962. 30-min increments.

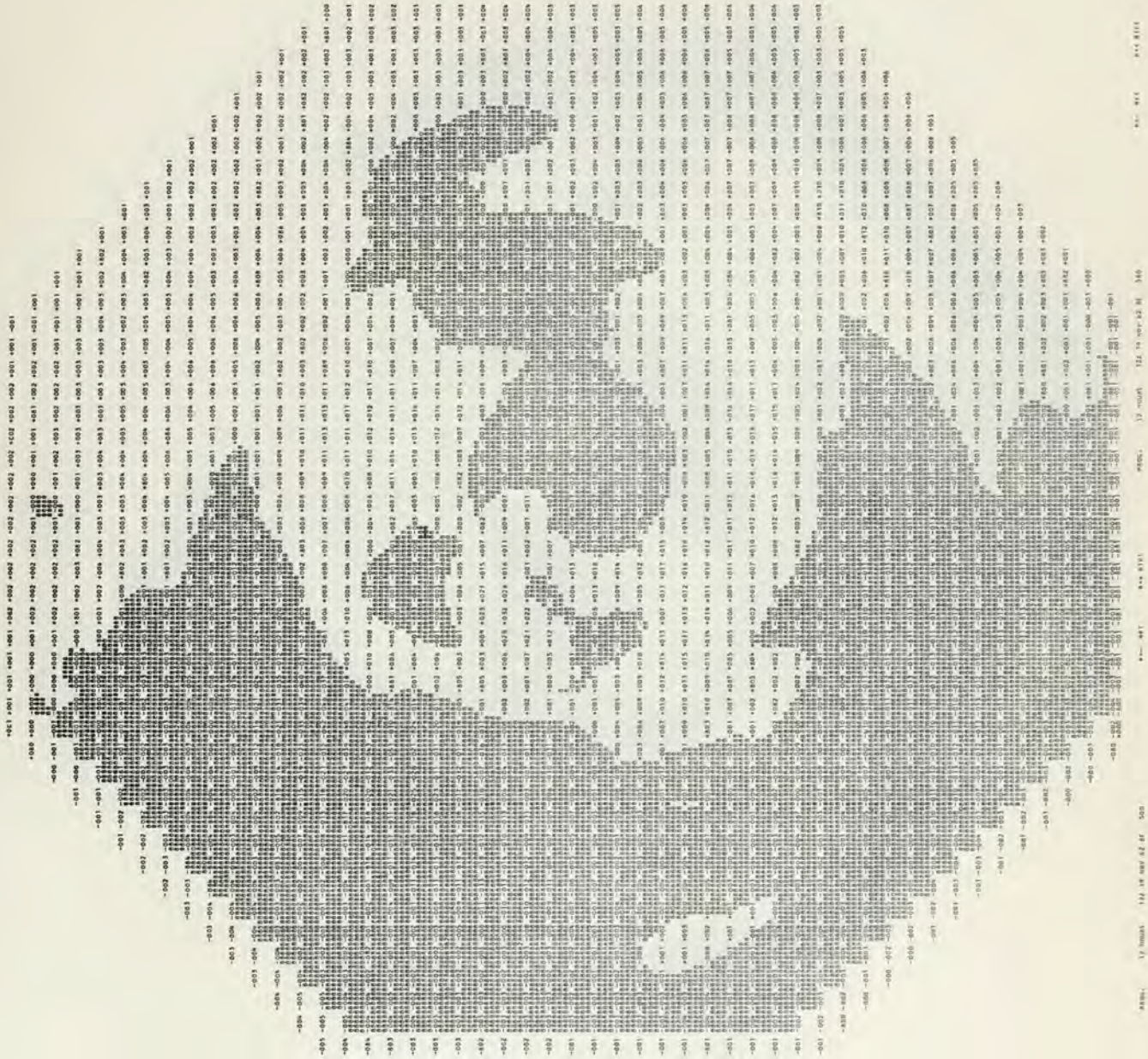

Figure 6 - 12-hr 500-mb planetary-scale height-change forecast for the Northern Hemisphere from 12Z 19 November 1962. 30-min increments.

Figure 7 - 12-hr 500-mb planetary-scale height-change analysis of the Northern Hemisphere from 12Z 19 November 1962.

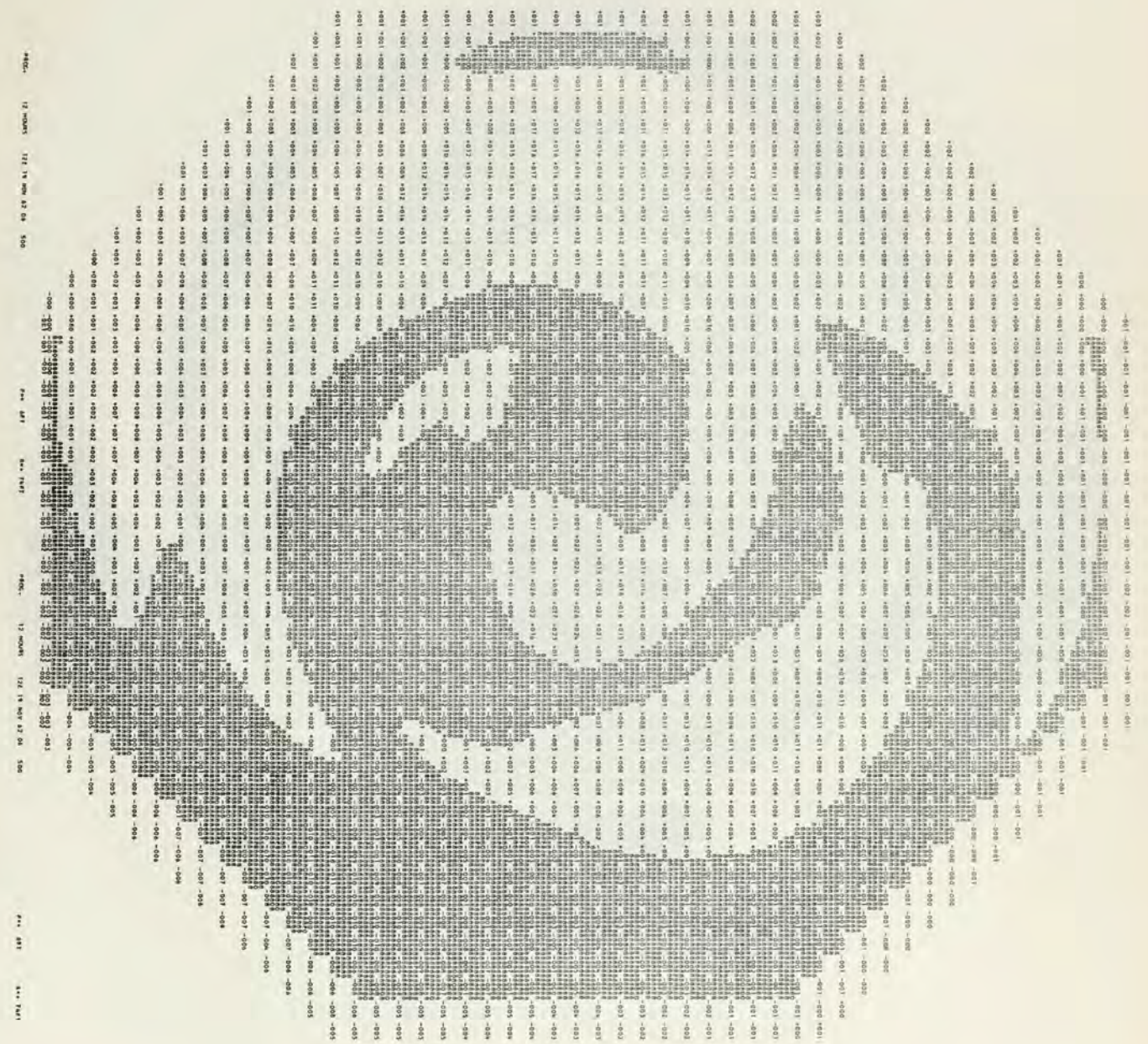

Figure 8 - 500-mb height analysis of the Northern Hemisphere after Fourier analysis. 00Z 20 November 1962.

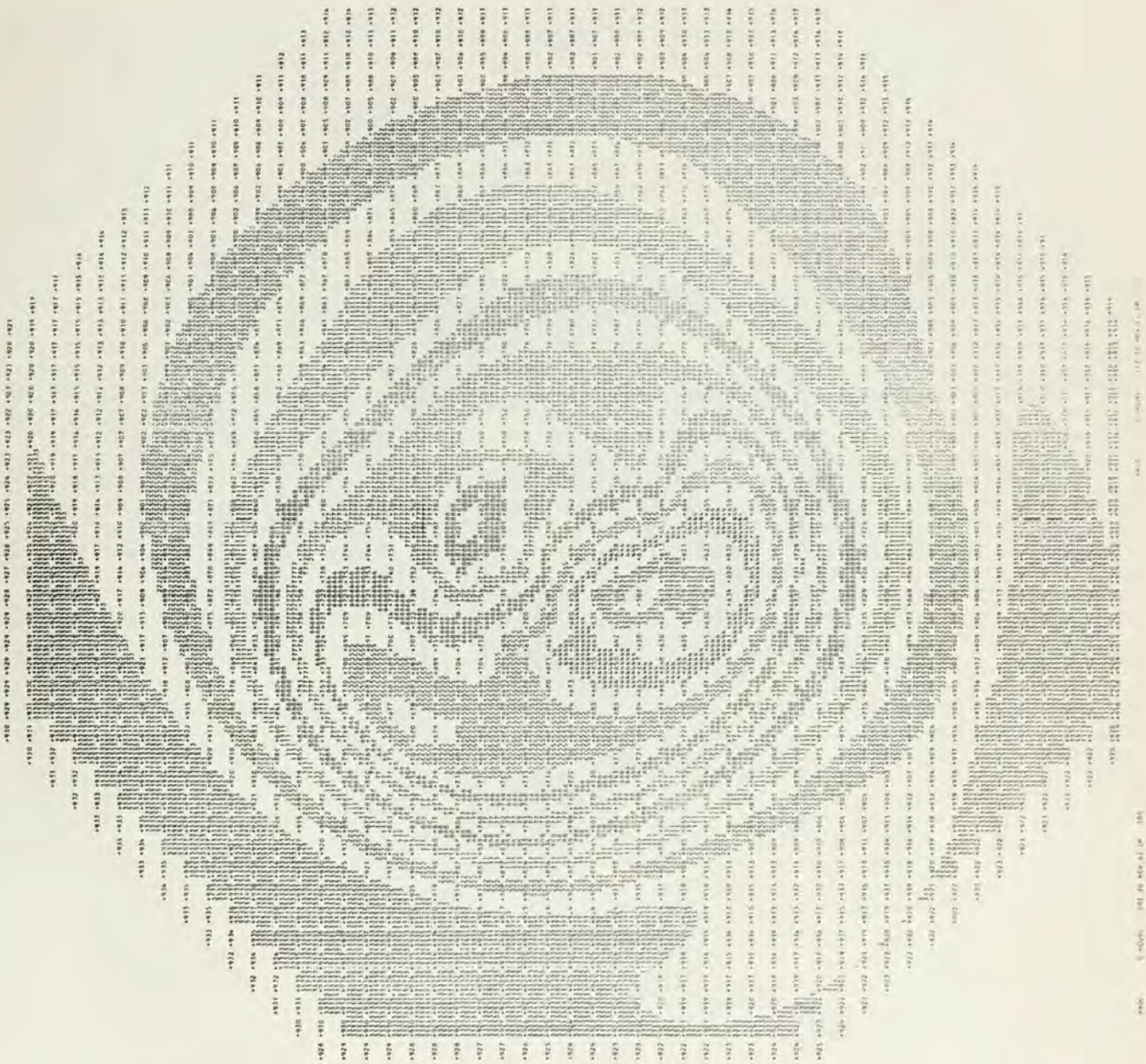

Figure 9 - Polar stereographic projection of the Northern Hemisphere to the scale of figs. 2 through 8.

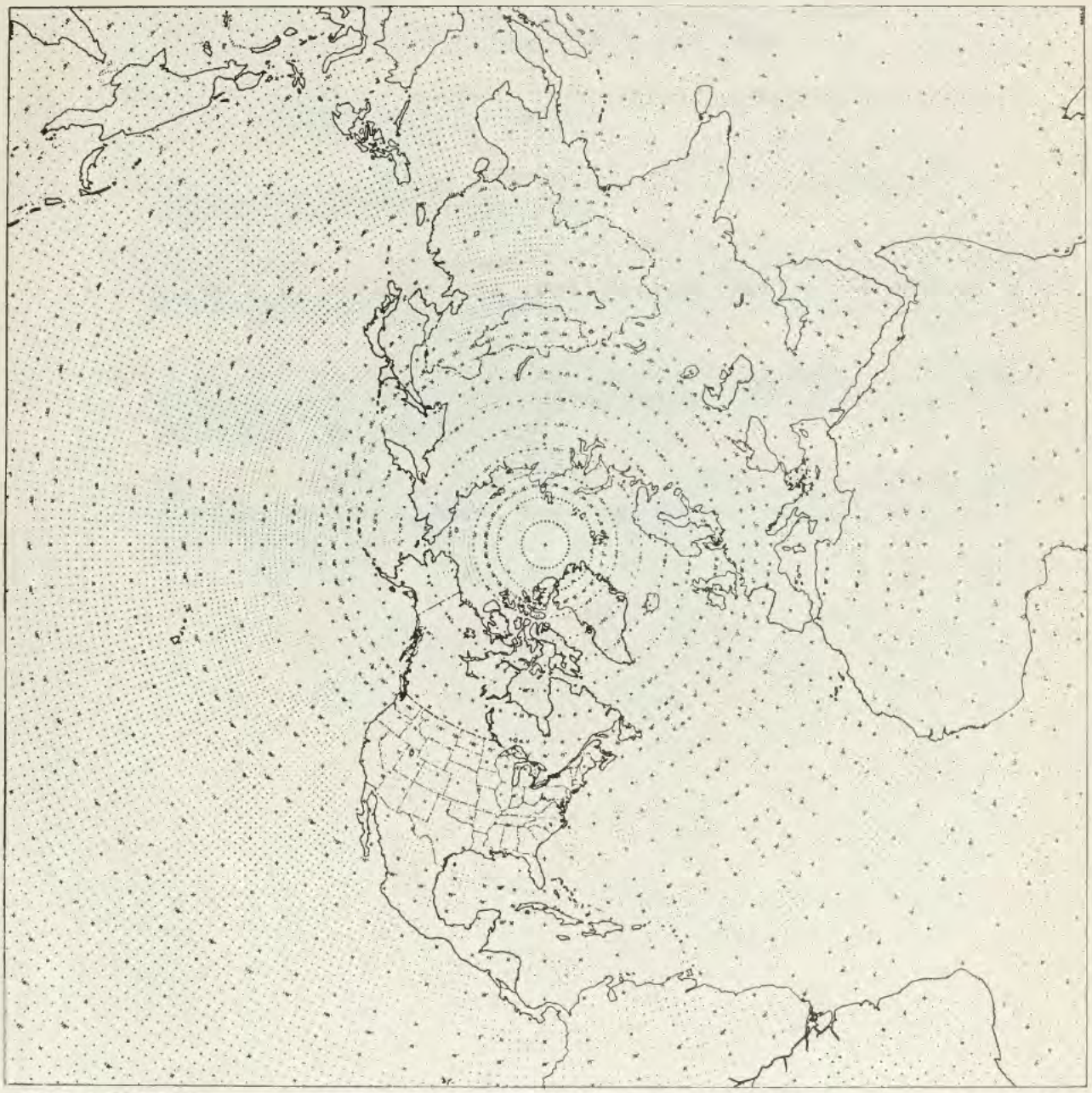

BIBLIOGRAPHY

1. Burger, A.P.: Scale considerations of planetary motions of the atmosphere, Tellus, vol. 10, No. 2, May 1959, pp. 195-205.

2. Holl, M. and J. Clark: Diagnostic cycle routine, Meteorology International, Inc., Monterey, California, May 1963.

3. Salvadori and Baron: Numerical methods in engineering, Prentice Hall, New York, 1952, pp. 47-49.

4. Thompson, P.D.: Numerical weather analysis and prediction, The MacMillan Company, New York, 1961.

5. Wiin-Nielsen, A.: On barotropic and baroclinic models, with special emphasis on the ultra-long waves, Monthly Weather Review, vol. 87, No. 5, May 1959, pp. 171-183.

6. Wiin-Nielsen, A.: A preliminary study of the dynamics of transient, planetary waves in the atmosphere, Tellus, vol. 13, No. 3, August 1961, pp. 320-333.

7. Wolff, P.M.: The error in numerical forecasts due to retrogression of ultra-long waves, Monthly Weather Review, vol. 86, No. 7, July 1958, pp. 245-250.

APPENDIX I

VERIFICATION OF PERSISTENCE FORECASTS
FOR SELECTED DAYS OF NOVEMBER 1962

Pillow is defined as

$$P = \frac{\sum_{n=1}^{x=n=1977} (A-B)_n}{x} \quad . \qquad \text{(I-1)}$$

The root-mean-square error (RMSE) is determined as follows:

$$RMSE = \sqrt{\frac{\sum_{n=1}^{x=n=1977} [(A-B)-P]_n^2}{x}} \quad . \qquad \text{(I-2)}$$

In equations (I-1) and (I-2), A_n and B_n represent the point values of the fields being compared. In this example, when preparing the data for these tables, the A-field was the analysis at the initial time and the B-field was at a subsequent time.

Index of Tables

Table format - Pillow / RMSE (values in feet)

Table I. Pillow and RMSE of persistence verifications at 5 levels for a 12-hr forecast during November 1962.

Initial Time	Level				
	300mb	500mb	700mb	850mb	1000mb
12Z 19	22/99	6/74	0/57	-2/50	0/61
00Z 20	-23/97	-9/68	3/54	2/57	-12/69
12Z 20	-11/88	-3/71	-3/63	0/66	10/74
00Z 21	1/96	5/74	4/51	4/45	7/50
12Z 22	4/87	5/61	5/48	7/42	6/50
12Z 23	0/90	5/76	-6/73	-3/71	5/68
00Z 24	-5/95	0/65	6/63	5/69	0/74
12Z 24	-3/97	-4/77	-7/71	-2/70	4/66

Table II. Pillow and RMSE of persistence verifications at 5 levels for a 24-hr forecast during November 1962.

Initial Time	Level				
	300mb	500mb	700mb	850mb	1000mb
12Z 19	-1/143	-3/96	2/77	0/89	-11/106
00Z 20	-35/122	-13/95	0/92	2/106	-1/116
12Z 21	-16/135	1/100	7/90	12/94	18/89
12Z 22	0/122	10/91	14/82	13/83	14/91

Table III. Pillow and RMSE of persistence verifications at 5 levels for 36, 48, 60 and 72-hr forecasts during November 1962.

Initial Time	Forecast Interval	Level				
		300mb	500mb	700mb	850mb	1000mb
12Z 19	36	-13/159	-6/115	0/116	0/130	0/155
12Z 22	36	0/139	5/140	7/134	10/133	20/139
12Z 19	48	-11/188	-1/147	4/137	4/150	6/171
12Z 22	48	-4/144	6/151	14/163	16/174	20/185
12Z 22	60	-8/178	1/188	7/203	13/208	24/213
12Z 22	72	-17/231	4/223	20/223	21/227	23/233